JETIR.ORG ISSN: 2349-5162 | ESTD Year : 2014 | Monthly Issue
JOURNAL OF EMERGING TECHNOLOGIES AND INNOVATIVE RESEARCH (JETIR)
An International Scholarly Open Access, Peer-reviewed, Refereed Journal

DNA interaction, molecular docking, anticancer, antimicrobial and thermal studies of binary cobalt complex of N-methylbenzylamine

Srinivas Kore[1,2], Sravanthi Maddikayala[3] Kavitha Bengi[4], and Saritha Reddy Pulimamidi *[1]

[1]Department of Chemistry, University College of Science, Osmania University, Hyderabad, Telangana State 500007, India.
[2]Department of Chemistry, Government Arts & Science College, Kamareddy, Telangana State 503111, India.
[3]Department of Chemistry, University College for Women, Osmania University, Koti, Hyderabad, Telangana State 500095, India.
[4]Department of Chemistry, Nizam College, Osmania University, Hyderabad, Telangana state 500001, India

Abstract:
The coordination behaviour of Cobalt (II) complex of N methylbenzylamine, $CoCl_2(Nmba)_2(H_2O)_2$ is reported. The structure and bonding of the metal complex has been deduced by analytical and spectral studies. Based on the above studies, the metal centre was found to be octahedral for Co(II) complex. The activation thermodynamic properties were calculated using the Coats–Redfern method. Thermal decomposition processes of complex are non-spontaneous; that is, the complex is thermally stable. The positive value of Gibbs free energy of decomposition (ΔG*) is non-spontaneous process. DNA binding properties of the metal complex, investigated using UV–visible absorption, fluorescence and viscosity measurement studies, unveiled a groove binding mode for the complex, with intrinsic binding constants (K_b) and Stern-Volmer quenching constant (K_{sq}) supporting its strong binding capabilities. Nuclease activity against pBR322 was assessed through gel electrophoresis. Additionally, docking studies using Autodock-4.2 software provided insights into their binding affinities. Biological studies revealed antimicrobial and cytotoxic activities of the complex.. Geometry optimization studies were performed. Molecular orbital calculations of the binary metal complex was computed by using accurate parametric model PM3 method.

Key words: DNA binding, Antimicrobial and Docking studies.

1. Introduction

In recent decades, there has been considerable interest in studying transition metal complexes with various amine ligands, particularly for their potential use in anticancer therapies targeting solid tumors. Research has shown that organic compounds with aromatic rings and amine side arms can intercalate with DNA. Additionally, further studies have revealed that metal coordination enhances DNA binding activity through metal-DNA base pair interactions [1].

Although several anticancer drugs have successfully treated certain cancer types, their effectiveness against solid tumors, such as breast cancer, has been limited. This limitation has led to an escalating demand for more potent treatments [2,3]. Consequently, cancer chemotherapy focusing on solid tumours has become a pivotal research area, necessitating the development of effective drugs. In this context, the selection of benzylamine derivatives as ligands for synthesizing Pt(IV) complexes and subsequently screening them for anticancer activity against the MCF-7 cell line represents a concerted effort to create efficient anticancer agents capable of reducing cytotoxicity[4]. Additionally, platinum complexes with benzylamine derivatives as ligands are utilized for their catalytic and biological applications.

Benzylamine-containing compounds have been investigated as potential therapeutic agents for a variety of ailments, including tuberculosis (TB) [5]. Research into their medicinal properties has explored their potential as antifungal and antibacterial treatments[6], and also best suited for anticancer[7] and anti-diabetic therapies[8]. Additionally, several benzylamine-containing drugs have already been approved for medical use. For instance, Pargyline is used to treat hypertension, and Butenafine serves as a topical antifungal medication. Based on the proven biological activities of benzylamine-containing compounds, here, we present our work on synthesis and characterisation of Co(II) complex of N-methyl benzylamine ligand followed by DNA interaction, molecular docking, anticancer, antimicrobial and thermal studies.

2. Procedure

2.1 Materials and methods:

All used reagent solutions and chemicals are of Analar grade (> 99.0%) and were bought from Merck,Sigma-Aldrich (Mumbai) India. Tumor cell lines(Hela,A549) were selected from NCCS Pune and the culture media RPMI1640 and DMEM from Sigma-Aldrich (Germany), Methyl thiazolyl diphenyl tetrazolium bromide (MTT) is from Sisco laboratory, Mumbai India. Calf Thymus-DNA was procured from Fluka stored at >20^{0}C. 2400 CHNS analyser (PERKIN-ELMER) was used for elemental analysis to know

their percentage in complex. Melting point(m.p) apparatus was used for determining the melting point(m.p) of the metal complex using open glass capillaries uncorrected. FT- IR spectra were achieved within 4000-400cm^{-1} range using potassium bromide (KBr) phase on IR (PERKIN-ELMER) spectrometer. Mass spectral studies were studied on Shimadzu Japan LCMS (2010) spectrometer. Digisun conductivity meter (Model -909) was used for obtaining conductance of the metal complex. DNA binding assay was carried out on UV(Shimadzu 160 A) absorption double beam spectrophotometer and FLUROMAX spectrofluorometer FP-8500 equipped with a xenon lamp using 1 cm path length rectangular quartz cuvette at 25 ºC for recording fluorescence emissions. Faraday Gouy's balance CAHN -7600 using Hg [Co (NCS)$_4$] as calibrant employed in studying Magnetic susceptibility moment(μ) of the complex. XRD powder studies were carried out in between 5^0 to 80^0 (2θ) using Rigaku Miniflex X-ray Diffractometer. Molecular modelling and energy optimization studies were done by using Chem3d pro software. Molecular Docking patterns of complexes were studied with Autodock-4.2 software and outcomes were visualized and analyzed using Biovia Discovery Studio Visualizer software.

2.2 Synthesis of the metal complex:

The metal complex was synthesized by the addition of methanolic (10ml) solution of N-methylbenzylamine ligand (10mmol, 0.12ml) drop wise to 10ml methanolic solution of the metal (II) salt [10mmol, 0.24gm of $CoCl_2.6H_2O$]. The contents were refluxed for 5-6 hrs on oil bath at about 70-80^0 C and the coloured precipitate separated out. The metal complex was filtered and washed using different solvents like ethanol, n-hexane, diethyl ether and double distilled water and left to dry overnight in vacuum. [9, 10, 11]The scheme for the synthesis of metal complex is given in **Figure-1**.

2.3 DNA binding studies:

UV-Vis absorption titrations were used to carry out DNA binding studies for the metal complexes, with fixed compound concentration (10 μM) while varying the CT-DNA concentration (0 - 100μM). Water was used as the first solvent for dissolving the metal complexes to get a compound stock solution. While measuring the absorption, small steady additions of CT-DNA were added to both the compound solution and the reference solution to remove the absorbance of CT-DNA itself and before absorption spectra was recorded the resulting compound solution was incubated for 5 minutes Upon data obtained, the binding constants (K_b) for all compounds were calculated using the following equation

$$\text{“ [DNA]}/(\varepsilon_a-\varepsilon_f) = [\text{DNA}]/(\varepsilon_b-\varepsilon_f) + 1/K_b(\varepsilon_b-\varepsilon_f)\text{”}$$

where [DNA]= deoxy ribonucleic acid concentration , ε_b=extinction coefficient for fully bound metal complex, ε_a= apparent extinction coefficient (= A_{obsd}/[complex]) and ε_f = extinction coefficient of free metal ion complex. K_b values were derived on substituting experimental data in the above equation. A plot of "[DNA]/ (ε_a -ε_f) vs [DNA]" gives a slope "1/(ε_a -ε_f)" and intercept "1/K_b (ε_a -ε_f)". K_b was calculated from the ratio of slope and intercept.

The fluorescence ethidium bromide (EthBr) displacement titrations were performed on spectrophotofluorometer in Tris-Hcl(pH 7.2) buffer with a fixed concentration of ethidium bromide (EthBr) of 40μM. The fluorescence spectra of EthBr-DNA complex was studied in the visible range between 525-750nm and the excitation wavelength fixed at 520nm. Quenching constant (K_{sv}) for determining the binding strength of the ligand and the derived complexes with calf thymus (CT-DNA) was obtained from the straight line slopes of *Stern- Volmer equation*:

$$\text{“}I_0/I = I + K_{sv}[r]\text{”}$$

Where I_0, I= emission intensity of EthBr-DNA in the absence and presence of quencher, K_{sv} = *Stern -Volmer* quenching constant, [r] = quencher (complex) concentration [12].

Viscosity assay using *Ostwald's* capillary viscometer maintained at 30±0.1^0 C was carried out, as optical photo physical techniques might not provide complete evidence for DNA binding. The CT-DNA concentration was 20μM and the concentration of the test compound varied from 0 to 100μM. Digital stopwatch was used to record mean flow time [13]. The recorded values were represented as $(\eta/\eta_0)^{1/3}$ vs [complex]/[DNA], where η and η_0 are the viscosities of CT-DNA solution with and without the complex present respectively. The data of viscosity was procured from the flow rate of CT-DNA compromising solutions (t) corrected from the flow rate of buffer alone (t_0). Equations "$\eta = (t_1 - t_0)/ t_0$ and $\eta_0 = (t - t_0)/ t_0$" were used to determine η and η_0 where t_0 = rate of flow of buffer alone, t = rate of flow of CT-DNA alone and t_1 = rate of flow of CT-DNA with the complex.

2.4 Gel electrophoresis studies

By using the agarose gel electrophoresis method, the metal complexes capacity to cleave DNA through photolytic investigations was calculated. In this test, metal complexes were applied to supercoiled pBR322 DNA at several quantities, and then the DNA was diluted with TrisHCl buffer at pH 7.2.The pre-treatment DNA-sample system was mixed with bromophenol blue (2 L) and then incubated for a further two hours at 37ºC. The samples were then loaded onto the wells of a 1% agarose gel that was set in a tray containing TAE buffer (pH 8.0) and electrophoresed for 45 minutes at 70 V. Before electrophoresis, the gel was treated with ethidium bromide. With the use of a BIO-RAD Gel documentation system, bands were seen under an ultraviolet (UV) trans illuminator and the gel that resulted was photographed (Aveli, 2021).

2.5 Biological assay

2.5.1 In vitro cytotoxicity and MTT studies:

MTT Assay is a colorimetric assay that measures the reduction of yellow 3-(4,5-dimethythiazol- 2-yl)-2,5-diphenyl tetrazolium bromide (MTT) by mitochondrial succinate dehydrogenase. The assay depends both on the number of cells present and, on the assumption, that dead cells or their products do not reduce tetrazolium. The MTT enters the cells and passes into the mitochondria where it is reduced to an insoluble, dark purple coloured formazan crystals. The cells are then solubilized with a DMSO and the released, solubilized formazan reagent is measured spectrophotometrically at 570 nm Cell viability was evaluated by the MTT Assay with three independent experiments with six concentrations of compounds in triplicates. Cells were trypsinized and performed the tryphan blue assay to know viable cells in cell suspension. Cells were counted by haemocytometer and seeded at density of 5.0 X 10^3 cells / well in 100 μl media in 96 well plate culture medium and incubated overnight at 37^{0}C. After incubation,

taken off the old media and added fresh media 100 µl with different concentrations of test extract in represented wells in 96 plates. After 48 hrs., Discarded the extract solution and add the fresh media with MTT solution (0.5 mg / Ml-1) was added to each well and plates were incubated at 37^0C for 3 hrs. At the end of incubation time, precipitates are formed as a result of the reduction of the MTT salt to chromophore formazan crystals by the cells with metabolically active mitochondria. The optical density of solubilized crystals in DMSO was measured at 570 nm on a micro plate reader. The percentage growth inhibition was calculated using the following formula.

$$\% \text{ Inhibition} = 100(\text{Control} - \text{Treatment})/\text{Control}$$

The IC50 value was determined by using linear regression equation i.e. y =mx+c. Here, y= 50, m and c values were derived from the viability graph.

2.5.2 In vitro Anti-microbial activity:

Bactericidal activity of the complexes synthesized was planned on two gram-negative bacterial strains (*Klebsiella* and *Pseudomonas*), two gram-positive bacterial strains (*Staphylococcus* and *Bacillus)*and two Fungal strains (*Candida and Aspergillus)*. The antibacterial assay was carried out by performing pour plate method in which 1% of active bacterial cultures were mixed into autoclaved agar media just before solidifying temperature and poured into the plates. After the plates were solidified, wells were made using sterile well borer and samples were loaded 100µl each into the wells respectively. Plates were incubated at 37 °C for 18-24 hours in a bacterial incubator. The antifungal assay was performed by using *Candida and Aspergillus*. Potato dextrose agar and Yeast Extract Peptone agar media were prepared and autoclaved. Just before pouring into the plates, antibiotic (Streptomycin/Chloramphenicol) was added into media to avoid bacterial contamination. The plates were allowed to solidify and 5mm wells were made using sterile well borer based on number of samples. The wells were loaded with 100µl of samples each. The plates were incubated at 25°C for 96 hours and results were noted[14].

2.3 Docking studies

Docking studies were conducted on synthesised metal-based complex using Autodock-4.2 software. Docking was carried out on crystal structure of Human DNA topoisomerase I (PDB_ID 1T8I), obtained from the Protein Data Bank. Molecular docking was performed with a 3D grid box (size: 50 x 66 x 50) centred at coordinates (x=22.45, y=-1.46, z=28.103). During the docking process, the default genetic algorithm was employed to generate 10 conformations for each ligand. Ligand and protein preparation were carried out using MGL tools-1.5.6, and the final docking was executed in Autodock-4.2 software.

The outcomes were visualized and analysed using Biovia Discovery Studio Visualizer software, facilitating a comprehensive understanding of the interactions between the ligands and the target protein. This approach enabled the exploration of potential binding modes and affinities of the synthesised metal complex towards Human DNA topoisomerase I, offering valuable insights into their potential as therapeutic agents.

3. Results and Discussions:

The synthesis of complex yielded satisfactory results with good yield, and is water soluble. Detailed physical parameters and elemental analyses of the complex are provided in **Table 1**. The composition of the complex was confirmed to be of the $Co(Nmba)_2$ type, as illustrated in **Figure 1** below.

Table 1: Physical and Analytical data of the binary metal complex

Complex with Emp. Formula	**Colour**	**Yield (%)**	**Melting Point (°C)**	**Molecular mass**	**$\Lambda_M(\Omega^{-1}\,cm^2\,mol^{-1})\times10^{-3}$**	**Micro analysis (Calculated)**			
						M	C	H	N
$[CoCl_2(Nmba)_2(H_2O)_2]$	Brown	75	>300	407	2.2	13.89 (14.09)	47.02 (47.07)	6.34 (6.42)	6.81 (6.86)

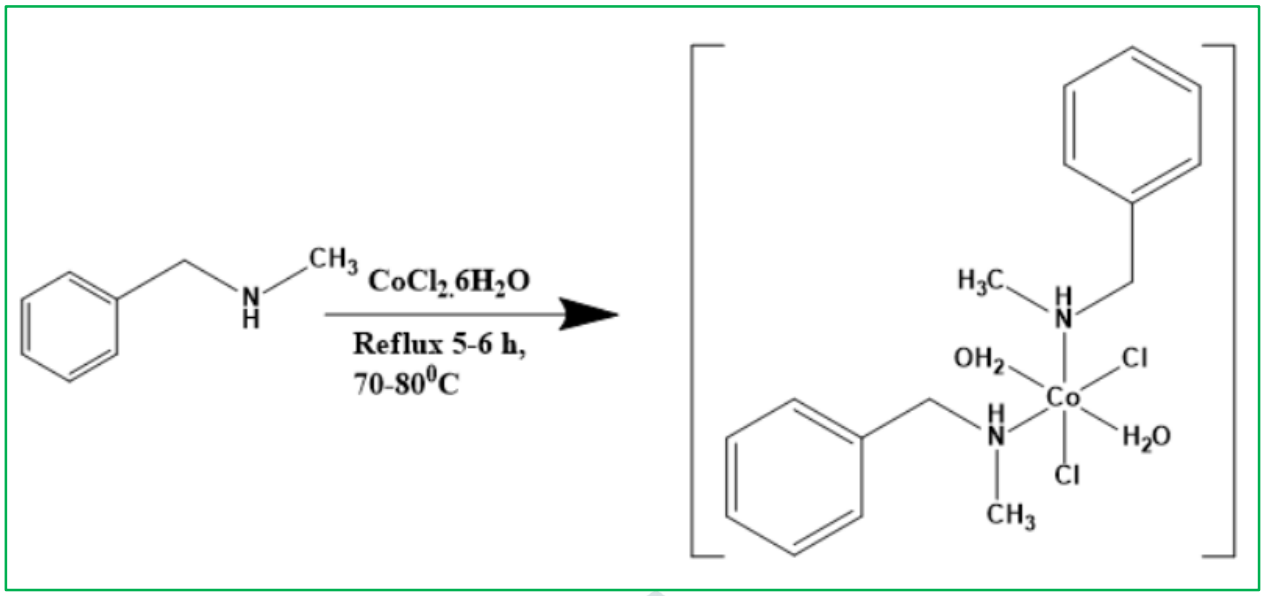

FIGURE 1: Synthesis scheme of the binary metal complex

3.1 Spectral characterization:

Molar conductance studies were undertaken to distinguish the electrolytic or non-electrolytic nature of the complex. [15] Findings revealed non electrolytic nature of the binary metal complex, with minimal conductance value of 2.2 Ω^{-1} cm^2 mol^{-1} $\times 10^{-3}$, indicating the presence of chloride ions within the coordination sphere.

Thermogravimetric analysis (TGA) and differential thermal analysis (DTA) curves for the binary complex is presented in **Figure 2**. TGA analysis of the complex exhibited a mass change of 8.84% indicative of the loss of two coordinated water molecule around 120-160°C. [16] The DTA curves for binary complex revealed endothermic peaks at about 110-120°C. In general, the complex displayed stability up to 350°C.

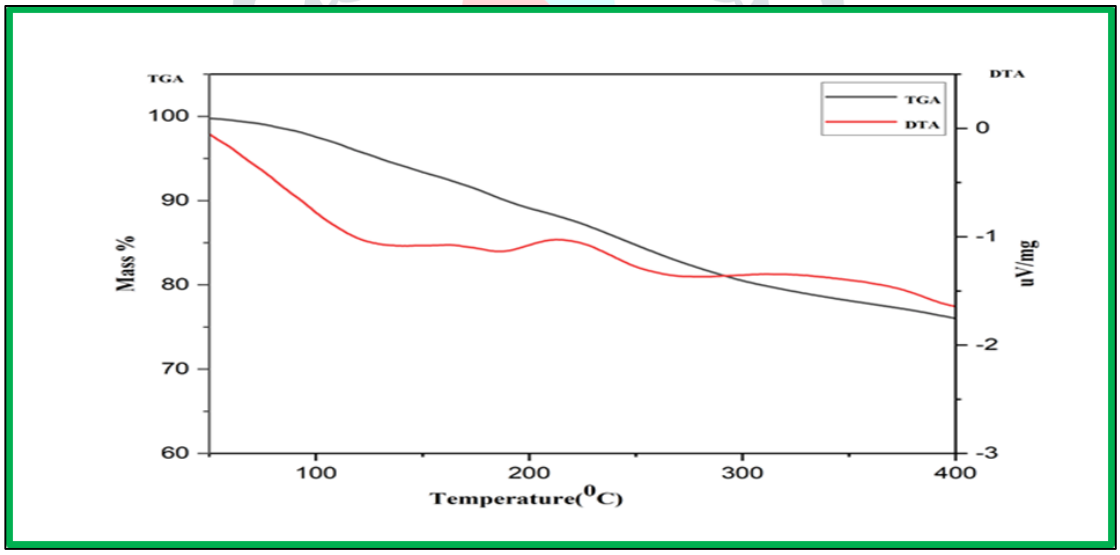

FIGURE 2: TGA and DTA spectra of binary metal complex

The IR vibrational stretching bands of the complex exhibit significant shifts compared to those of the ligand, indicating coordination. Coordination of N-methylbenzylamine by the nitrogen atom in the complex is demonstrated by the characteristic absorptions of the $–NHCH_3$ group, which appear around 3200-3400 cm^{-1} (ϑNH), 2923 cm^{-1} (ϑasyCH_3).[17] In addition, the absorption band at 1303 cm^{-1} due to $\delta NH + \delta CH_3$ mode in the free ligand, exhibits a shift to lower frequency of 1216 cm^{-1} supporting coordination.[18] Intensive bands at 723 cm^{-1} in complex, indicate the presence of mono-substituted phenyl rings through out-of-plane C-H bending vibrational modes. Medium intensity bands around 330-482 cm^{-1} indicate the presence of ν (M-N) and ν(M-Cl) vibrations.[18,19] This suggests that both N-methylbenzylamine ligands coordinate to the metal ion through nitrogen donor atoms. The IR stretching frequencies of the synthesized binary complex is displayed in **Table 2** and **Figure 3**.

Table 2: Tabulated IR frequencies of the synthesized binary complex

Compound	υ(NH) cm^{-1}	υ(CH3) cm^{-1}	υ(C=C)(phenyl) cm^{-1}	υ(C-N) cm^{-1}	Mono substituted Phenyl cm^{-1}	υ(M-N) cm^{-1}	υ(M- Cl) cm^{-1}
$[CoCl_2(Nmba)_2(H_2O)_2]$	3318 3360	2923	1505	1216	723	482	330

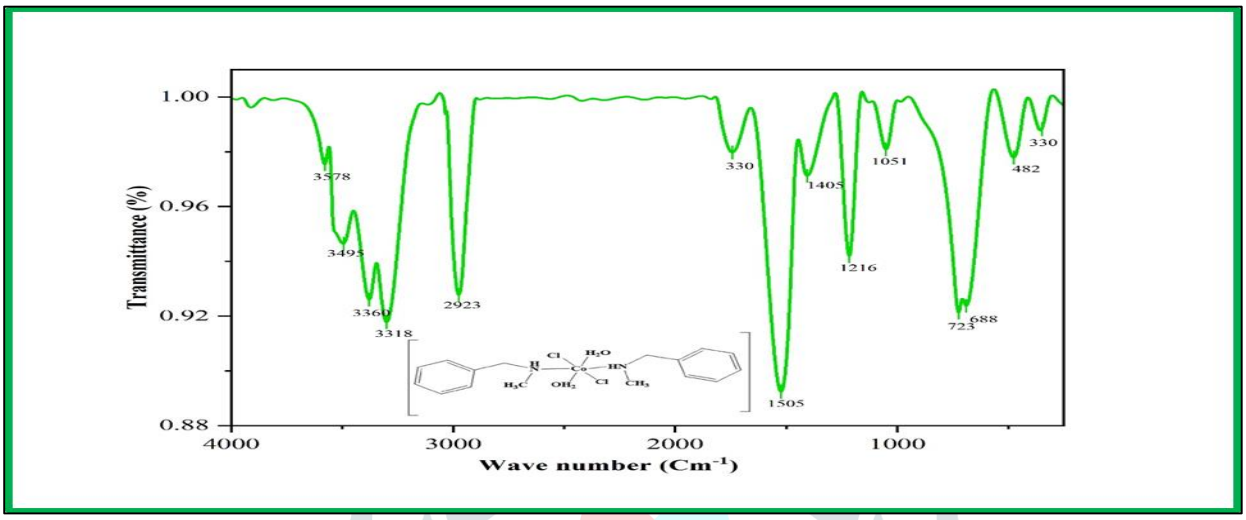

Figure 3: IR spectrum of Co(II) complex

The LC-MS spectra, obtained at room temperature, displayed peak at m/z 407 for the metal complex and displayed in **Figure 4**. Analysis of the mass spectrum confirmed the correctness of the proposed molecular formula.

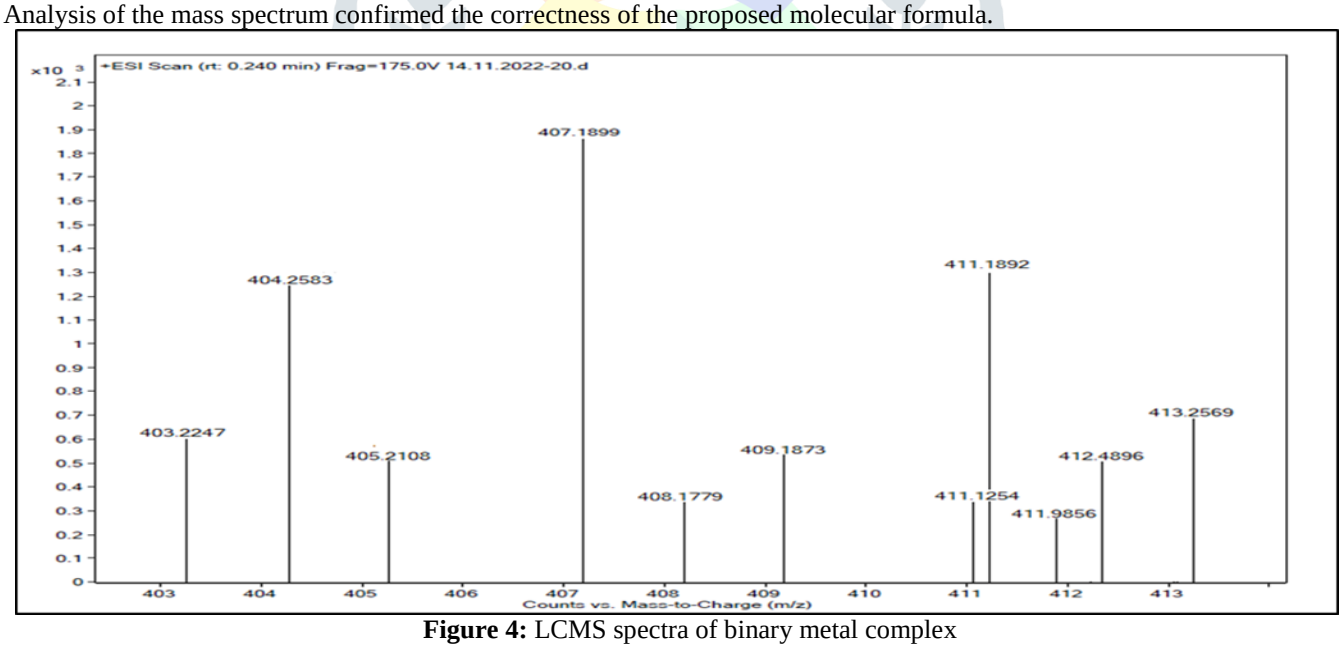

Figure 4: LCMS spectra of binary metal complex

The magnetic moment value of 2.94 BM for the metal complex is in good agreement with the expected values in octahedral geometry.

The electronic transition bands at 15,220 $cm^{-1}(\nu_1)$, 18,726 $cm^{-1}(\nu_2)$ and 26,041 $cm^{-1}(\nu_3)$ in the cobalt complex indicate "$^4T_{1g}(F) \rightarrow {}^4T_{2g}(F)$ (ν_1), $^4T_{1g}(F) \rightarrow {}^4A_{2g}(F)$ (ν_2) and $^4T_{1g}(F) \rightarrow {}^4T_{1g}(P)$ (ν_3)" transitions respectively in a octahedral geometry. The magnetic susceptibility value of 2.94 BM also supports this. [20] The presence of low transition band at 28,571 and 31,847 cm^{-1} suggests CT transitions in the complex. The ratio of ν_2 to ν_1 is 1.23 is shown in **Table-3**, close to the octahedral structure, confirms its geometry.

The ligand field parameter (Dq), Nephelauxetic ratio represented as β and Racah parameter B are calculated using Kong's equations. For the metal complex, the Racah parameter (B) is 312 cm^{-1}, which is lower than that of the free ion value, indicating

an overlap of metal-ligand orbitals and suggests the presence of covalent bonding. [21] Similarly, the Nephelauxetic ratio (β) range is 0.32, further indicating a covalent character. Electronic spectra of the synthesized complex is shown in **Figure 5**.

Table 3: Magnetic and UV-Vis spectral data of binary metal complex

Compound	Mag. moment μ_{eff} (B.M)	Absorption cm^{-1}	Band Assignment	υ_2 / υ_1	$\upsilon 3 / \upsilon 1$	Dq, cm^{-1}	β	B cm^{-1}	Proposed Geometry
$CoCl_2(Nmba)_2(H_2O)_2$	2.94	15,220 18,726 26,041 28,571 31,847	$^4T_{1g}(F) \rightarrow {}^4T_{2g}(F)$ (ν_1) $^4T_{1g}(F) \rightarrow {}^4A_{2g}(F)$ (ν_2) $^4T_{1g}(F) \rightarrow {}^4T_{1g}(P)$($\nu_3$) Charge transfer band Charge transfer band	1.23	1.71	350	0.32	312	Octahedral

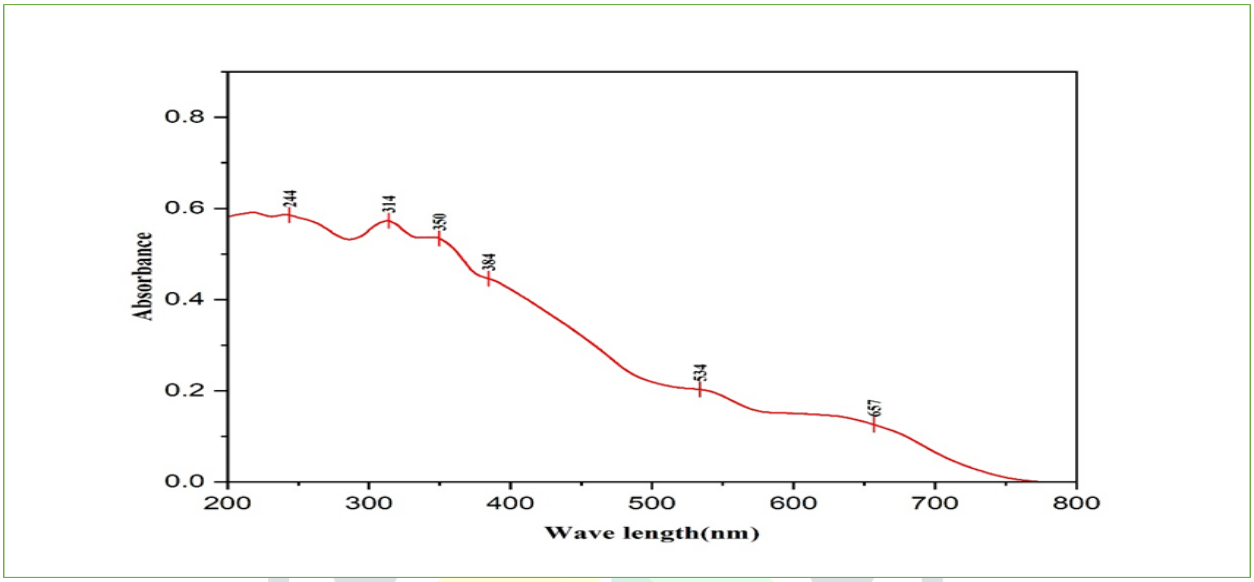

Figure 5: Electronic spectra of binary metal complex

The powder XRD patterns, crucial for the structural characterization of the metal complex, was examined within the 2θ range of 50 to 800. [22] These spectra exhibit distinct crystalline patterns, each with differing degrees of crystallinity, as illustrated in **Figure 6**.

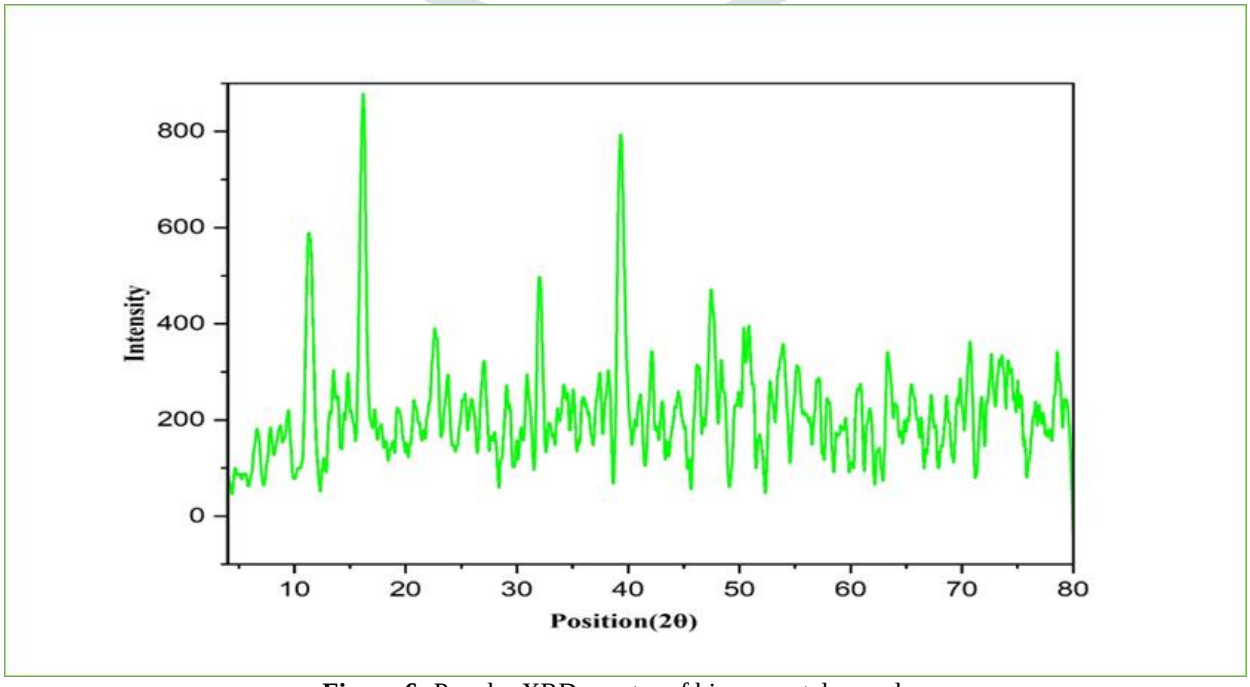

Figure 6: Powder XRD spectra of binary metal complex

3.2 Geometry optimization structures of metal complexes:

The geometry optimization of the synthesized complex was conducted using Chem3D Pro Ultra software, focusing on bond lengths and bond angles, as outlined and elaborated upon in **Table 4**. The observed changes in planarity in the optimized structures of the complex is attributed to ligand coordination with the metal centre. **Figure 7** illustrates the HOMO-LUMO orbitals for metal complex. Various parameters, including the HOMO-LUMO energy gap (ΔE), S, global softness, absolute hardness represented as η, ΔNmax (additional electronic charge), chemical potential (μ), global electrophilicity represented as ω, χ (absolute electronegativity) and absolute softness (σ) were calculated and are provided in **Table 4**. [23] ΔE indicates kinetic stability or chemical reactivity. For the binary metal complex, the value of ΔE is 2.635 eV. Furthermore, the electrophilicity value of the metal complex surpasses that of the free ligand, suggesting increased reactivity. It can be emphasised that cobalt complex is highly polarizable, exhibiting less kinetic stability and high reactivity, classifying it as a "soft" molecule.

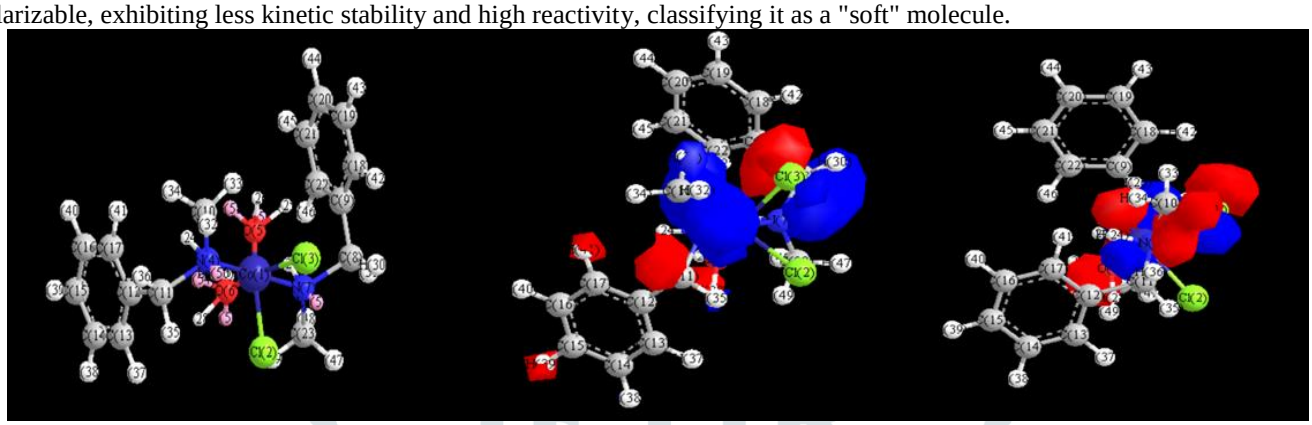

FIGURE 7: HOMO – LUMO orbitals of the binary metal complex

Table 4: Calculated quantum parameters of the complex

COMPLEX	HOMO	LUMO	ΔE	χ	σ	μ	s	ω	ΔNmax	η
$[CoCl_2(Nmba)_2(H_2O)_2]$	-8.94	-6.305	2.635	7.622	0.75901	-7.622	0.37951	22.0503	5.7856	1.3175

3.3 Kinetic parameters:

The change in the activation energy (ΔE), change in entropy represented as ΔS, change in enthalpy as ΔH and Gibbs free energy change ΔG of the complexes were determined to elucidate their decay process. These thermodynamic parameters were determined using the Coats-Redfern (CR) relation, and the calculated values are presented in **Table 5 (Figure 8)**. [24] A high activation energy value indicates higher thermal stability of the complex. The reaction is non spontaneous, as indicated by positive ΔG and negative ΔS reading indicates more ordered activated complex than reactants. Based on the ΔH values, reactions can be described as endothermic ($\Delta H > 0$) or exothermic ($\Delta H < 0$). They can also be categorized as endergonic or exergonic depending on free energy changes. [25, 26]A best fit with a linear function is indicated by the correlation coefficients, which range is 0.9958, derived from the Arrhenius plots of the title compounds. Hence, it can be suggested that synthesised binary metal complex exhibit thermal stability, non-spontaneous behaviour, and are endothermic in nature.

Complex	Stage	Parameters					
		E (J mole^{-1})	A (S^{-1})	ΔS (J mole^{-1} K^{-1})	ΔH (J mole^{-1})	ΔG	R^2
$[CoCl_2(Nmba)_2(H_2O)_2]$	I	$2.27x10^4$	$1.95x10^7$	$-1.09x10^2$	$1.84x10^4$	$7.52x10^4$	0.9958

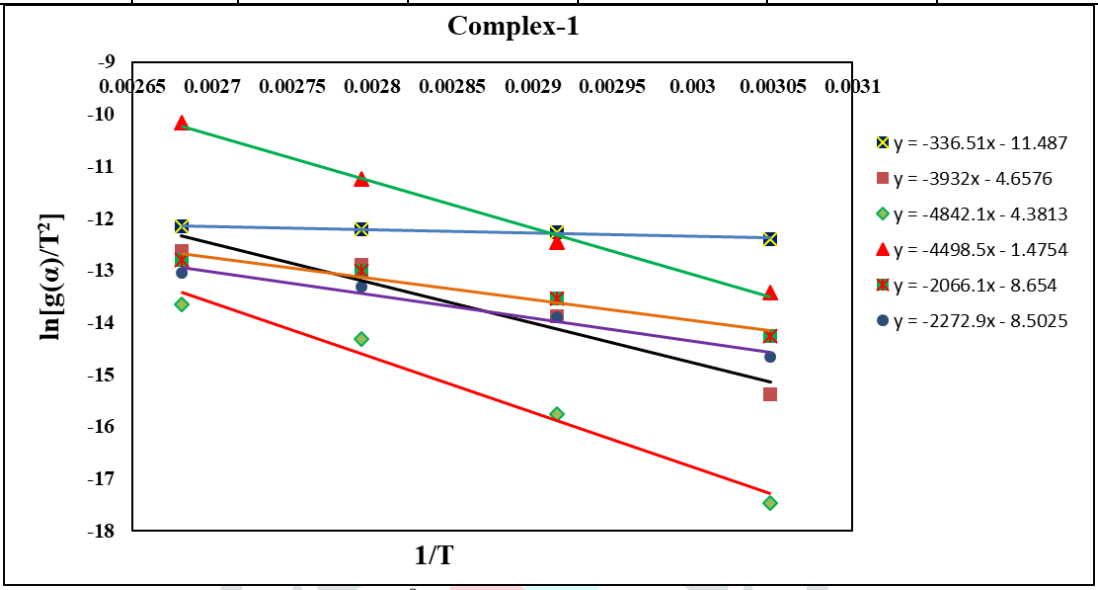

FIGURE 8: Plots of $\ln[g(\alpha)/T^2]$ vs 1/T of complex for different Coats-Redfern models

Table 5: Kinetic parameters using Coats-Redfern (CR) relation for binary metal complex

3.4. DNA interaction studies

3.4.1 Absorption studies:

Electronic absorption titration is a valuable technique for studying DNA binding, as it provides insights into changes in intensity and spectral shifts of charge transfer bands as DNA concentration varies. Synthesised binary metal complex exhibits hyperchromism with a slight redshift in the presence of DNA **(Figure 9)**. This complex likely interacts with double-stranded DNA through diverse modes dictated by its structure, charge and ligand composition. Hydrogen bonding sites are available in both minor and major grooves of the DNA double helix. The NH groups of the binary complex may probably bind to nitrogen of adenine or oxygen of thymine in DNA through hydrogen bond, thereby contributing to the observed hyperchromism in the recorded absorption spectra. [27] Additionally, the hyper chromic effect might result from an electrostatic interaction between the positively charged complex and the negatively charged phosphate backbone located on the outer edge of the DNA double helix. [28] The binding constant (Kb) for complex, determined as $3.3x10^5$ M^{-1}, indicates its significant binding affinity towards CT-DNA. The intrinsic binding constant (Kb) is affected by factors like the planarity of the complex, the presence of electron-donating or electron-withdrawing groups on the ligand, and additional hydrogen bonding. The observed binding constants are consistent with groove binding, as documented in the literature. [29-31] consequently, our findings suggest that the synthesized complexes likely engage in DNA binding via groove binding. [32]

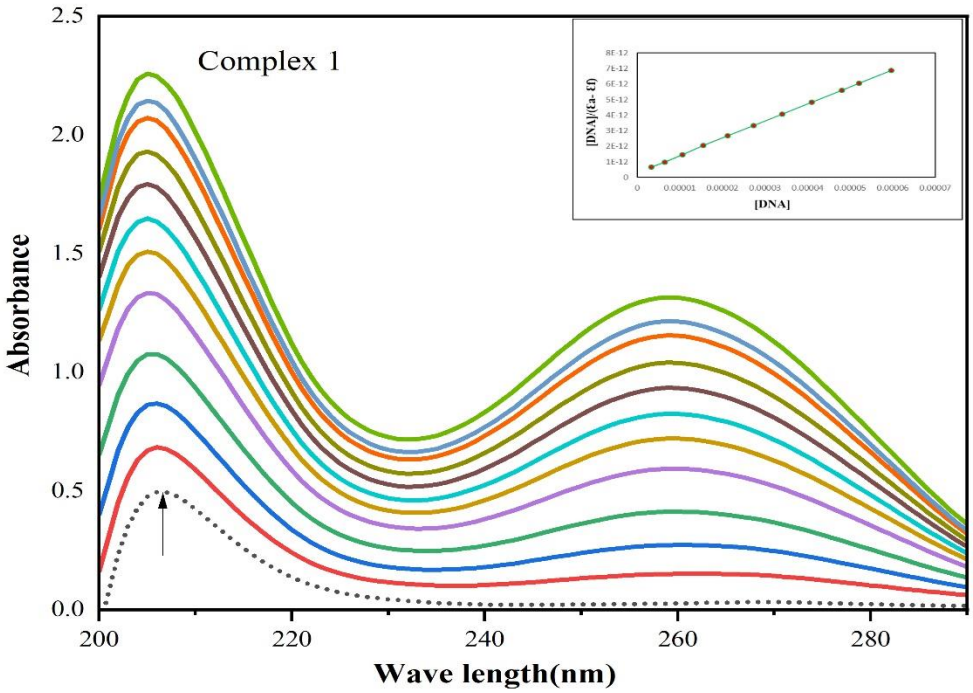

FIGURE 9: UV-Vis spectra of complex [10μM] on addition of CT-DNA[10-100μM]. Arrow(↑) depictsabsorbance upon adding increasing concentration of CT-DNA.Inset:[DNA]/($\varepsilon_a - \varepsilon_f$)vs [DNA].

3.4.2 Fluorescence emission studies:

Fluorescence quenching experiments were carried out to assess the DNA binding ability of the complex compared to ethidium bromide (EB). It is well established that free ethidium bromide shows diminished emission intensity in a Tris-HCl buffer due to solvent quenching. In contrast, EB exhibits strong fluorescence when intercalated between base pairs of DNA, while this process can be reversed by the introduction of competing agents. **Figure 10** illustrates the quenching curves for DNA bound ethidium bromide, both with and without the complex. A significant decrease in emission intensity has been observed on addition of the complex to DNA bound EB indicating their interaction with CT-DNA through groove binding. [33] Stern-Volmer equation was used for further analysis of the data. The quenching plots (**Figure 10**) demonstrate that the fluorescence quenching of DNA bound ethidium bromide by the complexes aligns linearly with the Stern-Volmer relationship, confirming the binding of the complex to DNA. Typically, when the compound binds to DNA through intercalation mode, the emission intensity of the system decreases by more than 50%, considering the ratio of the compound concentration to DNA is less than 100. [34] From the figure it is evident that, addition of the synthesized complex to the DNA-EB system, decreases the intensity by less than 50%, which further supports that the complexes bind to DNA through groove binding. Results obtained from the Stern-Volmer equation plot of "I_0/I vs [complex]/[DNA]" revealed Ksv value for synthesised metal complex as 1.24×10^6 M^{-1}. Both K_b and Ksv data indicate similar binding affinities of the synthesised metal complex to CT-DNA.

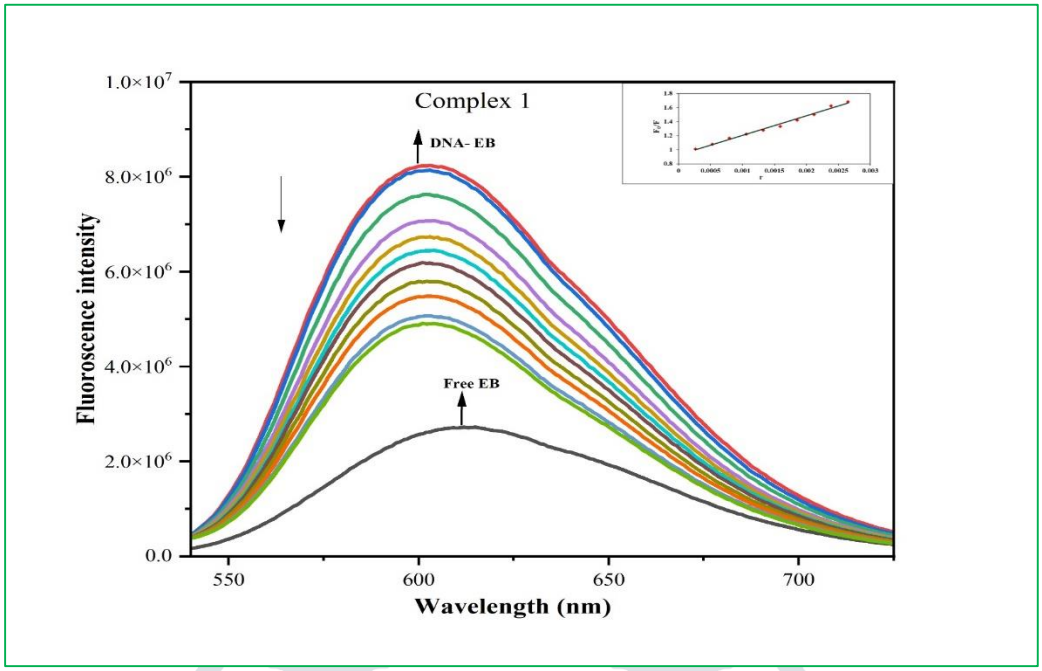

FIRURE 10: Fluorescence spectrum of complexes at varied concentration [10-100 µM] on EB[40µM] -DNA[130µM] complex.The arrow (↓)depicts the decrease in intensity on increasing the conc. of the complex. Inset: I_0/I vs [complex].

3.4.3 Viscosity titrations:

In the classical intercalation model, an increase in DNA viscosity can occur as the DNA helix lengthens due to the separation of base pairs to accommodate the binding ligand. [35] However, in cases of partial or non-classical intercalation model of interaction between DNA & ligand, the ligand may cause bending or kinking of the DNA helix, thereby shortening its effective length and consequently, its viscosity. Ligands that exclusively bind within the DNA grooves tend to induce relatively minor alterations in DNA solution viscosity under identical conditions. [36] The gradual increase in relative viscosity of CT-DNA observed with increasing amounts of the complex as seen in **Figure 11** supports groove binding. [37] This phenomenon could be attributed to alterations in either flexibility or conformation of DNA or solvation of the DNA molecule.

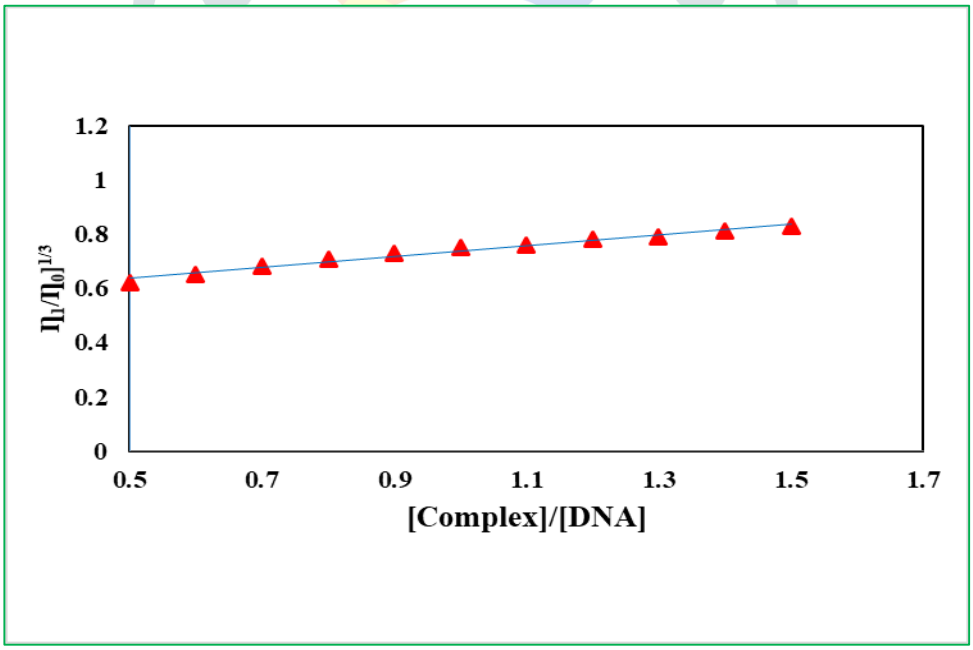

FIGURE 11: Changes in viscosity on increasing concentrations of complex [0-100µM] and CT-DNA [20µM] investigated at a controlled temperature of 30±0.10°C, within a 5mM Tris-HCl buffer solution.

3.5 DNA nuclease studies

The DNA nuclease activity of the synthesized complex, which can be correlated with in vitro cytotoxicity was investigated using agarose gel electrophoresis. The incorporation of the metal ion into the polymer typically enhances nuclease activity. [38] **Figure 12** illustrates the DNA cleaving ability of synthesised complex.

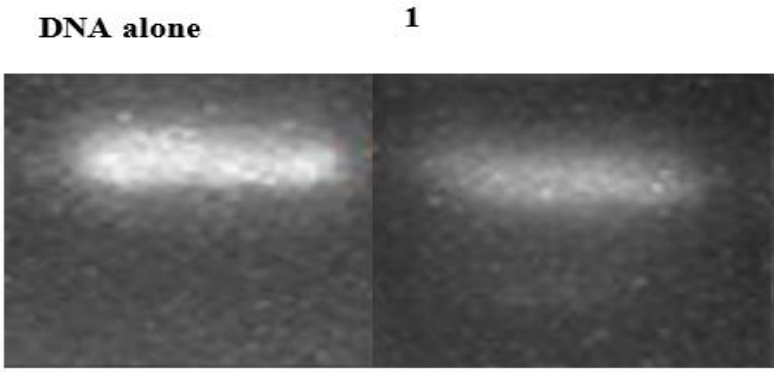

FIGURE 12: Photo cleavage studies of pBR322 DNA, with and without binary metal complex with concentration range of 20µM.

3.6 Biological studies

3.6.1 Antimicrobial activity:

The antimicrobial properties of the synthesized binary metal complex were investigated using the agar disc diffusion method against bacterial and fungal cultures. Results indicate that the complex exhibited enhanced activity, a phenomenon elucidated by Overtone's concept. [39] The antimicrobial effects were evaluated by measuring the zone of inhibition, as seen in **Figures 13 and 14**.[40] Additionally, the bar diagram illustrating the biological activity of the synthesized complex, presented in **Figures 15 and 16**, demonstrates the order of the activities of the complexes under study as shown in **Table 6 and 7** .

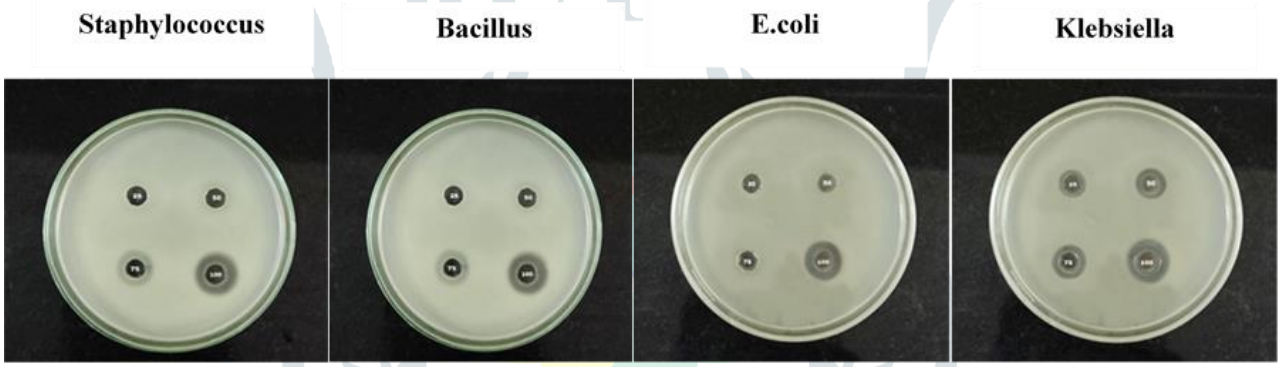

FIGURE 13 : Antibacterial images of binary metal complex

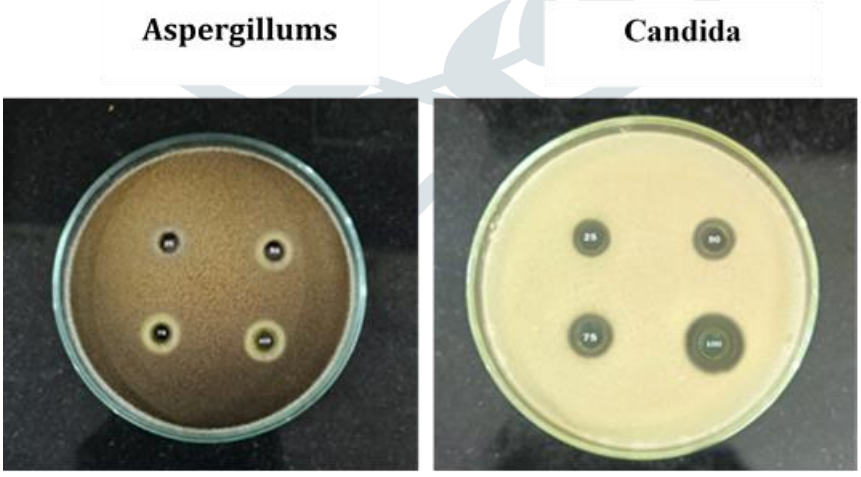

FIGURE 14: Antifungal images of binary metal complex

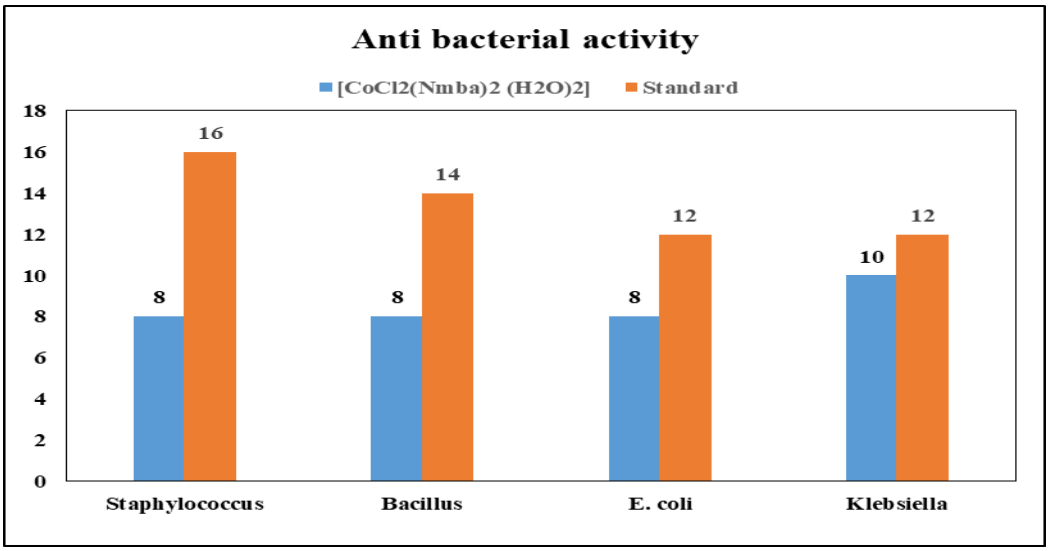

FIGURE 14: Bar diagram of Antibacterial activity of binary metal complex

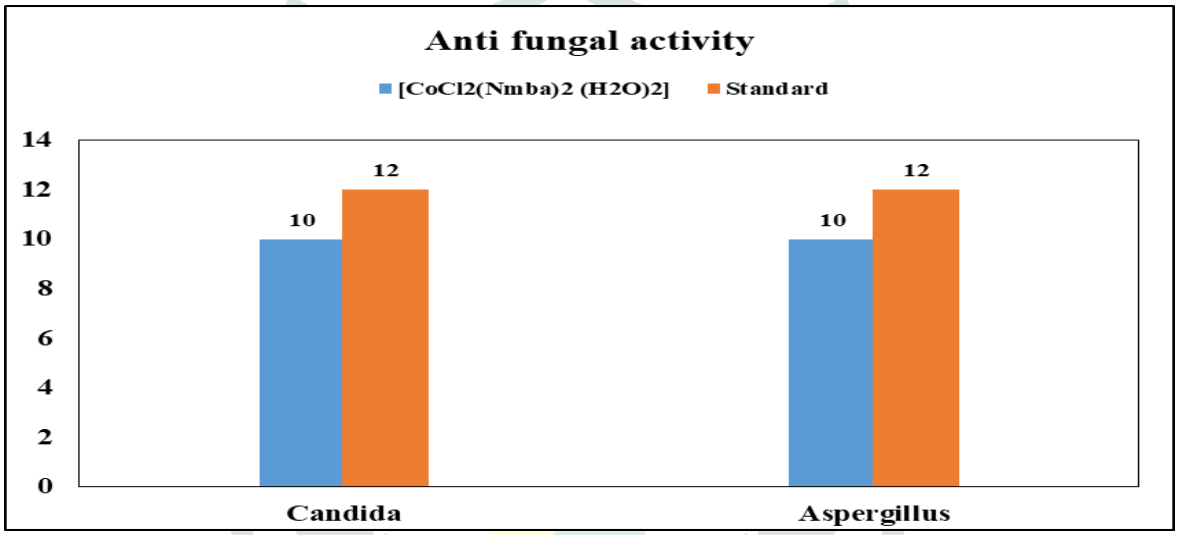

FIGURE 15: Bar diagram of Antifungal activity of binary metal complex

Table 6: Zone of inhibition (mm) of the binary metal complex against bacterial strains at 10mg/mL concentration

Compound	Bacterium (Zone of inhibition (mm)			
	Gram positive		Gram Negative	
	Staphylococcus	Bacillus	E. coli	Klebsiella
$[CoCl_2(Nbma)_2(H_2O)_2]$	8	8	8	10
Standard (Streptomycin)	16	14	12	12

Table 7: Zone of inhibition (mm) of the binary metal complex against fungal strains at 10mg/mL concentration

Compound	Candida	Aspergillus
$[CoCl_2(Nbma)_2(H_2O)_2]$	10	10
Standard (Candida – Fluconazole)	12	12

3.6 Docking studies

Autodock 4.2 software was employed to elucidate the binding strengths of the compounds with DNA and the receptor protein utilized was human DNA Topoisomerase I (PDB ID: 1T8I). [41] The studies reveal that synthesised metal complex exhibited the highest binding affinity of -10.87 kcal/mol towards the active site of the receptor protein (**Figure 16**). The results of docking studies are listed in **Table 8.**

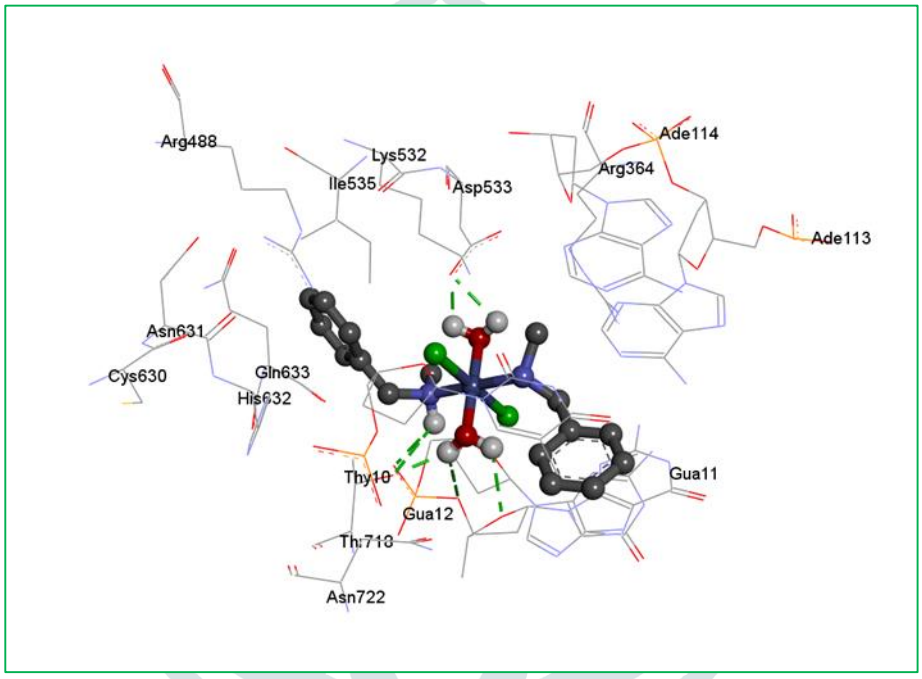

FIGURE 16: The docking images of the synthesized complex (ball models) within the active binding site of the human DNA topoisomerase I protein.

Table 8: Docking results of the complex

S.No	Binding affinity (in Kcal/mol)	vdW + H bond + desolv Energy (in Kcal/mol)	Electrostatic Energy (in Kcal/mol)	No. of Hydrogen bonds	H-bond distance (in Å)
$[CoCl_2(Nmba)_2(H_2O)_2]$	-10.87	-11.66	-1.4	Thr718:OG1 – LIG:H28 Gua12:OP1- LIG:H28 Asp533:OD2 – LIG:H26 Asp533:OD2- LIG:H27 Gua11:O4'-LIG:H24 Thr718:OG1 - LIG:H25 Gua11:O3' – LIG:H25	2.875 2.172 2.209 1.867 2.403 1.99 3.032

4. Conclusion

This paper presents the synthesis of Co(II) complex of N-methylbenzylamine, its characterization through various analytical and spectroscopic techniques and exploration of the DNA interaction and biological activities. Elemental analysis and mass spectral studies reveal the stoichiometry of the complex as 1:2 of metal salt and ligand. Spectral analysis proposes octahedral geometry around the metal ion for the synthesized complex. CT-DNA binding studies, conducted via UV-Visible absorption studies, revealed a hyper chromic shift with intrinsic binding constants (Kb) of the order $10^5\,M^{-1}$. Both absorption and fluorescence quenching studies indicate groove mode binding activity. Nuclease studies demonstrated the efficacy of the complex in DNA cleavage. Biological assays revealed considerable antibacterial and antifungal activities for the binary metal complex. The formation of significant hydrogen bonds between the metal complex and amino acid residues of human topoisomerase I protein suggests good binding and stability.

ACKNOWLEDGEMENT

The authors express their gratitude to the OU DST_PURSE Program for financial support and to the Department of Chemistry, UCS, OU and GASC (A) Kamareddy for providing laboratory infrastructure through the DST-FIST programs.

CREDIT AUTHOR STATEMENT

Mr. Srinivas Kore was responsible for conceptualization, data curation, formal analysis, investigation, methodology development, resource acquisition, and drafting the original article. Dr. M. Sravanthi and Dr. B. Kavitha handled visualization and computational tasks. Prof. P. Saritha Reddy provided supervision, validation, and final manuscript editing. All authors contributed to and shaped the final version of the manuscript.

DECLARATION OF COMPETING INTEREST

The authors declare no known competing financial interests or personal relationships that could have appeared to influence the work reported in this paper.

DATA AVAILABILITY STATEMENT

The spectral data used to characterize the ternary metal complexes, which support the findings of this study, are provided in the supplementary information of this article.

ORCID

Srinivas Kore https://orcid.org/0009-0000-9153-4574

Sravanthi Maddikayala https://orcid.org/0000-0001-6891-6048

Kavitha bengi https://orcid.org/0000-0001-6891-6048

Saritha Reddy Pulimamidi https://orcid.org/0000-0003-4800-9568

REFERENCES:

[1]. L. Jiazheng, G. Haiwei, Z. Xiandong, Y. Zhang, P. Zhao,J. Jiang and L. Zang, Synthesis and characterization of unsymmetrical oxidovanadium complexes: DNA-binding, cleavage studies and antitumor activities, *J. Inorg. Biochem.,* 2012, 112, 39–48.

[2]. H. Bakr and E. Nassan, Synthesis, antitumor activity and SAR study of novel [1,2,4]triazino[4,5-*a*]benzimidazole derivatives *Eur. J. Med. Chem*., 2012, 53, 22–27.

[3]. D. M. Parkin and L. M. Fernandez, Use of Statistics to Assess the Global Burden of Breast Cancer, *Breast J.,* 2006, 12,S70–S80.

[4]. Sahra Lemos, Silmar J S Franchi, Adelino VG Netto and Antonio Eduardo Mauro, Synthesis, characterization, thermal studies, and DFT calculations on Pd(II) complexes containing N-methylbenzylamine. *Journal of Thermal Analysis and Calorimetry*, November 2011. DOI: 10.1007/s10973-011-1494-9

[5]. Cai, S.; Zhu, G.; Cen, X.; Bi, J.; Zhang, J.; Tang, X.; Chen, K.; Cheng, K. Synthesis, structure-activity relationships and preliminary mechanism study of N-benzylideneaniline derivatives as potential TLR2 inhibitors. *Bioorg. Med. Chem.,* **2018**, *26*(8), 2041-2050.

[6]. Ameta, R.K.; Singh, M.; Kale, R.K. Synthesis and structure–activity relationship of benzylamine supported platinum(iv) complexes. *New J. Chem.*, 2013, 37(5), 1501-1508.

[7]. Mojena, M.; Povo-Retana, A.; González-Ramos, S.; Fernández-García, V.; Regadera, J.; Zazpe, A.; Artaiz, I.; Martín-Sanz, P.; Ledo, F.; Boscá, L. Benzylamine and thenylamine derived drugs induce apoptosis and reduce proliferation, migration and metastasis formation in melanoma cells. *Front. Oncol.*, **2018**, *8*(AUG), 328.

[8]. Ameta, R.K.; Singh, M.; Kale, R.K. Synthesis and structure–activity relationship of benzylamine supported platinum(iv) complexes. *New J. Chem.*, **2013**, *37*(5), 1501-1508.

[9]. Rakesh Kumar Ameta, Nitin Kumar Sharma , Chetan B Sangani and Man Singh Synthesis, Characterization, Thermal, DNA binding, DFI, Antioxidant and Anticancer Studies of Bis (methylphenylmethanamine) Dichloroplatinum Complex. *Int J Chem Sci*. **2017**;15(3):152

[10]. Sahra C. ,Lemos Silmar J. S. Franchi , Adelino V. G. Netto , Antonio E. Mauro ,Oswaldo Treu-Filho , Regina C. G. Frem , Eduardo Tonon de Almeida , Cla´udia Torres Synthesis, characterization, thermal studies, and DFT calculations on Pd(II) complexes containing N-methylbenzylamine *J Therm Anal Calorim* (**2011)** 106:391–397. DOI 10.1007/s10973-011-1494-9

[11]. B. Kavitha , M. Sravanthi , P. Saritha Reddy, DNA interaction, docking, molecular modelling and biological studies of o-Vanillin derived Schiff base metal complexes, *Journal of Molecular Structure 1185* **(2019**) 153e167, https://doi.org/10.1016/j.molstruc.2019.02.093.

[12]. M .Gaber, HAEI-Ghamry, SK.Fathalla,*Spectrochim Acta A.***(2015),**139,396.

[13]. Kunche Sudeepa, Nagula Narsimha, Boinala Aparna, Sivan Sreekanth, A.V.Aparna,

[14]. Pulimamidi Rabindra Reddy, Suryam Rajeshwar, Battu Satyanarayana, Synthesis, characterization of new copper(ii)Schiff base and 1,10 phenahroline complexes and study of their bioproperties, *Journal of Photochemistry & Photobiology B*, 160(2016)217-224, doi: 10.1016/j.photobiol.2016.017.

[15]. Pulimamidi Rabindra Reddy, Suryam Rajeshwar, Battu Satyanarayana, Synthesis, characterization of new copper(ii)Schiff base and 1,10 phenahroline complexes and study of their bioproperties, *Journal of Photochemistry & Photobiology B*, 160(2016)217-224, doi: 10.1016/j.photobiol.2016.017.

[16].N.Kavitha,P.V.AnanthaLakshmi,Synthesis,characterization and thermogravimetricanalysis of Co(II), Ni(II), Cu(II) and Zn(II)complexes supported by ONNO tetradentate Schiffbase ligand derived from hydrazino benzoxazine, *Journal of Saudi Chemical Society* (**2017**)21, S457–S466 http://dx.doi.org/10.1016/j.jscs.2015.01.00.

[17]. Sahra C. Lemos , Silmar J. S. Franchi , Adelino V. G. Netto , Antonio E. Mauro ,Oswaldo Treu-Filho, Regina C. G. Frem, Eduardo Tonon de Almeida, Cla´udia Torres. Synthesis, characterization, thermal studies and DFT calculations of Pd(II) complexes containing N-Methylbenzylamine. *J Therm Anal Calorim* (**2011)** 106:391–397. DOI 10.1007/s10973-011-1494-9.

[18]. Pulimamidi Saritha Reddy,P.V.Ananthalakshmi and V.Jayatyagaraju, Synthesis and Structural Studies of First Row Transition Metal Complexes with TetradentateONNO Donor Schiff Base Derived from 5-Acetyl2,4-dihydroxyacetophenone and Ethylenediamine, *E-Journal of Chemistry*(**2011**), 8(1), 415-420.

[19]. Kavitha Bengi, Sravanthi Maddikayala, Saritha Reddy Pulimamidi, Biological evaluation, molecular docking, DNA interaction and thermal studies of new bioactive metal complexes of 2-hydroxybenzaldehyde and fluorobenzamine Schiff base ligand ,*Appl Organomet Chem*. **2020**;e6085, https://doi.org/10.1002/aoc.6085.

[20]. Sravanthi Maddikayala, Kavitha Bengi, Saritha Reddy Pulimamidi, DNA interaction, molecular dynamics simulation, molecular docking, biological, in vivo anti-inflammatory and thermal studies of o-hydroxyacetophenone and 2-fluoroaniline Schiff base complexes, *Appl Organomet Chem*. **2022**;e6839, https://doi.org/10.1002/aoc.6839.

[21]. Kavitha Bengi,Sravanthi Maddikayala,Saritha Reddy Pulimamidi, DNA binding, cleavage, docking, biological and kinetic studies of Cr(III), Fe(III), Co(II) and Cu(II) complexes with ortho-vanillin Schiff base derivative, *Appl Organomet Chem*. **2021**;e6451. https://doi.org/10.1002/aoc.6451.

[22]. P. Vasantha, B. Sathish Kumar, B. Shekhar, P.V. Anantha Lakshmi, Cobalt(II)–metformin complexes containing α-diimine/α-diamine as auxiliary ligand: DNA binding properties, *Appl Organometal Chem*. **2017**;e4074. https://doi.org/10.1002/aoc.4074.

[23].Bhushan Nazirkar, Mustapha Mandewale & Ramesh Yamgar, Synthesis, characterization and antibacterial activity of Cu (II) and Zn (II) complexes of 5- aminobenzofuran-2-carboxylate Schiff base ligands, *J. Taibah. Univ. Sci*. **(2019)**, 13, 440-449, https://doi.org/10.1080/16583655.2019.1592316.

[24].S. F. Sousa, G. R. P. Pinto, A. J. M. Ribeiro, J. T. S. Coimbra, P. A. Fernandes, M. J. Ramos, Comparative Analysis of the Performance of Commonly Available Density Functionals in the Determination of Geometrical Parameters for Copper Complexes*J. Comput. Chem.* **2013**, 34, 2079. https://doi.org/10.1002/jcc.23349.

[25].N. Kavitha, P. V. Anantha Lakshmi, Transition metal complexes supported by ONNN/ONNS bis-bidentate benzoxazine Schiff base: Synthesis, characterization, geometry optimization and non-isothermal kinetic parameters *J. Mol. Struct*. **2019**,1176, 798, https://doi.org/10.1016/j.molstruc.2018.09.042

[26]. A. Mumtaz, T. Mahmud, M. R. Elsegood, G. W. Weaver, Synthesis and Characterization of New Schiff Base Transition Metal Complexes Derived from Drug Together with Biological Potential Study*J. Nucl. Med. Radiat. Ther*. **2016**, 7, 6. https://doi.org/10.4172/ 2155-9619.1000310.

[27]. H. Chao, W. -J. Mei, Q. -W. Huang, DNA binding studies of ruthenium(II) complexes containing asymmetric tridentate ligands ,*J. Inorg. Biochem*. **2002**,92, 165.

[28] Y. N. Xiao, C. X. Zhan, Studies on the interaction of DNA and water-soluble polymeric Schiff base–nickel complexes *J. Appl. Polym. Sci.* **2002**, 84, 887. https://doi.org/10.1002/app.10000.

[29].F. Arjmand, F. Sayeed, Synthesis, characterization and DNA-binding studies of mono and heterobimetallic complexes $CuSn_2$/$ZnSn_2$ and their DNA cleavage activity,*J. Mol. Struct*. **2010**, 965, 14.

[30] S. Sharma, S. Singh, K. M. Chandra, D. S. Pandey, DNA-binding behavior of ruthenium(II) complexes containing both group 15 donors and 2,2′:6′,2″-terpyridine*J. Inorg. Bio-chem*. **2005**, 99, 458.

[31] Q. L. Zhang, J. G. Liu, J. Liu, G. Q. Xue, DNA-binding and photocleavage studies of cobalt(III) mixed-polypyridyl complexes containing 2-(2-chloro-5-nitrophenyl)imidazo [4,5-f][1,10]phenanthroline *J. Inorg. Biochem*.**2001**, 85, 291.

[32]. Nitesh Kumar, Raj Kaushal, Pamitha Awasthi. Non-Covalent binding studies of transition metal complexes with DNA. Journal of Molecular Structure. Vol. 1288, 15 sep 2023, 135751.

[33]. J. E. N. Dolatabadi, V. PanahiAzar, A. Barzegar, A. A. Jamali,F. Kheirdoosh, S. Kashanian, Y. Omidi, Spectroscopic and molecular modeling studies of human serum albumin interaction with propyl gallate *RSC Adv.* **2014**, 4, 64559.

[34]. Mozhgan Khorasani-Motlagh, Meissam Noroozifar, Asieh Moodi, Sona Niroomand ,Fluorescence studies, DNA binding properties and antimicrobial activity of a dysprosium(III) complex containing 1,10-phenanthroline, *J. of Photochem and Photobiology B: Biology* Vol. 127, 5 October 2013, Pages 192-201.

[35]. M. B. Gholivand, S. Kashanian, H. Peyman, H. Roshanfekr, DNA-binding study of anthraquinone derivatives using Chemometrics methods, *Eur. J. Med. Chem.* 2011, 46, 2630. https://doi.org/10.1016/j.ejmech.2011.03.034

[36] F. Arjmand, M. Aziz, DNA-binding study of anthraquinone derivatives using Chemometrics methods. *Eur. J. Med. Che*m. **2009**, 44, 834., https://doi.org/10.1016/j.ejmech.2011.03.034.

[37] P. X. Xi, Z. Xu, X. H. Liu, F. J. Chen, Z. Z. Zeng, X. W. Zhang,Y. Liu, Synthesis, Characterization, Antioxidant Activity and DNA-Binding Studies of Three Rare Earth (III) Complexes with 1-(4-Aminoantipyrine)-3-tosylurea Ligand, *J. Fluoresc*. **2009**, 19, 63.

[38]. Shanta Dhar, Munirathinam Nethaji, and Akhil R. Chakravarty, DNA Cleavage on Photoexposure at the d−d Band in Ternary Copper(II) Complexes Using Red-Light Laser, *Inorg. Chem*. **2006**, 45, 11043−11050, https://doi.org/10.1021/ic060328e.

[39]. Kavitha Bengi, Sravanthi Maddikayala, Saritha Reddy Pulimamidi, DNA binding, cleavage, docking, biological and kinetic studies of Cr(III), Fe(III), Co(II) and Cu(II) complexes with ortho-vanillin Schiff base derivative, *Appl Organomet Chem*. **2021**;e6451. https://doi.org/10.1002/aoc.6451.

[40].K.Rajeshwari, P.V. Anantha Lakshmi,J. Archana,M. Sumakanth,Ternary Cobalt(II), Nickel(II), and Copper(II) complexescontaining metformin and ethylenediamine: Synthesis,characterization, thermal, in vitro DNA binding, in silicomolecular docking, and in vivo antihyperglycemic studies, *Appl Organomet Chem.* **2020**;e6100. https://doi.org/10.1002/aoc.6100.

[41]. K Rajeshwari , P Vasantha , B Shekhar , P V Anantha Lakshmi Metformin-Derived Water-Soluble Cobalt Complexes: Thermal, Spectroscopic, DNA Interaction, and Molecular Docking Studies, *Appl Biochem Biotechnol*. **2022** Jun;194(6):2650-2671.doi: 10.1007/s12010-022-03862-3.